JACS
JOURNAL OF THE AMERICAN CHEMICAL SOCIETY

Communication

pubs.acs.org/JACS

Orthogonal Ternary Functionalization of a Mesoporous Metal–Organic Framework via Sequential Postsynthetic Ligand Exchange

Chong Liu, Tian-Yi Luo, Evan S. Feura, Chen Zhang, and Nathaniel L. Rosi*

Department of Chemistry, University of Pittsburgh, 219 Parkman Ave., Pittsburgh, Pennsylvania 15260, United States

Supporting Information

ABSTRACT: A sequential postsynthetic ligand exchange process was used to prepare a series of mono-, di-, and trifunctionalized mesoporous metal–organic frameworks (MOFs). Using this process, orthogonal functional groups were installed and thereafter postsynthetically modified with dye and quencher molecules. Microspectrophotometry studies were used to determine the distribution of the two orthogonal functional groups within the MOF crystals.

The properties of complex systems rely on the precise organization of functional molecular subunits in three-dimensional (3D) space. Typically, these subunits are found within a larger molecular architecture that serves as a scaffold for organizing the subunits with respect to one another. The scaffold structure and the individual molecular subunits are equally important in defining system properties.

Metal–organic frameworks (MOFs)[1] are ideal scaffold materials for organizing molecules in 3D space. Multiple different approaches have been developed for installing complex functional moieties onto MOF scaffolds, which have led to rapid expansion of MOF diversity.[2] These methods, which include postsynthetic modification and postsynthetic ligand exchange, allow introduction of functional groups that are often incompatible with the solvothermal reaction conditions typically used for MOF synthesis. Multiple postsynthetic ligand modification reactions have been reported, including condensation reactions, cycloaddition reactions, and metalation.[3] To date, these have allowed for installation of up to two different functional moieties in a single MOF.[4] Ligand exchange is also a powerful method of tuning MOF composition, functionality, and porosity.[5] These two strategies can be used in tandem to further increase the diversity and complexity of MOFs.[6]

Both the porosity and the structure of the scaffold MOF affect the level of complexity achievable from both postsynthetic ligand modification and ligand exchange methods. For example, microporous MOFs are ideal scaffolds for organizing relatively "small" functional moieties in close proximity to one another. New selective sorbents and complex heterogeneous catalysts have been created via postsynthetic modification of microporous MOFs.[7] Mesoporous MOFs, on the other hand, are ideal scaffolds for organizing relatively "large" functional species, because the pore dimensions allow for facile entry and diffusion of larger and more complex molecules.[8] In terms of structure and bonding, most reported MOFs have a single ligand strut connecting neighboring metal clusters (Figure 1A). If multiple ligands link neighboring clusters (Figure 1B), one can imagine

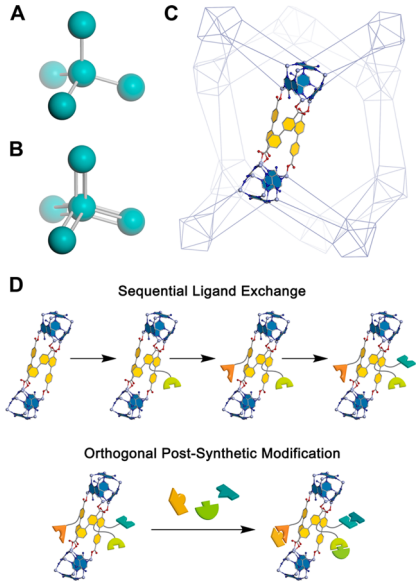

Figure 1. (A) Representation of metal nodes linked by single-ligand structs. (B) Representation of metal nodes linked by multiple-ligand struts. (C) In bMOF-100, discrete zinc-adeninate clusters are connected together by three-BPDC bundles in the extended framework, which is represented here by its underlying network. (D) Sequential ligand exchange process for installing multiple orthogonal functional groups and subsequent covalent modification of functional groups.

closely arranging multiple different functional groups, facilitating interactions between these groups that could lead to cooperative functionality. Having ligand clusters connecting neighboring metal clusters may be especially important for mesoporous MOFs, in which ligands surrounding the mesopores are spaced far apart. Such motifs would allow one to install functional groups in close proximity to one another in a mesoporous MOF. In 2012, we reported mesoporous bMOF-100, a structure consisting of zinc-adeninate vertices interconnected through a bundle of three 4,4′-biphenyldicarboxylate (BPDC) linkers (Figure 1C) rather than a single ligand bridge.[9] We demonstrated that it could be postsynthetically modified with large and complex molecules and that its porosity could be systematically increased via stepwise ligand exchange reactions.[5p,10] The three-ligand bundle motif connecting the vertices coupled with the large mesopores presents the unique opportunity to employ sequential ligand exchange reactions to

Received: June 30, 2015
Published: August 10, 2015

DOI: 10.1021/jacs.5b06780
J. Am. Chem. Soc. 2015, 137, 10508–10511

install up to three different functional moieties in very close proximity in 3D space (Figure 1D) and thereafter use these moieties as sites for covalently attaching large complex molecules via postsynthetic ligand modification.

Here, we report the installation of three orthogonal functional groups into the bMOF-100 scaffold. We subsequently show that these functional groups can be postsynthetically modified with large dye and quencher molecules, illustrating the level of structural and functional complexity that can be achieved within this system. The degree of completion and the relative ease of ligand exchange can depend on the lability of the metal−ligand bond within the MOF.

Our previous studies have shown that bMOF-100 is amenable to facile and nearly quantitative ligand exchange reactions.[5p] In this study, we aimed to replace BPDC with BPDC linkers functionalized at the 2-position to introduce new functionality to the pore space. Within the framework, the 2-carbon positions on the biphenyl struts are ≤7.5 Å from each other. We synthesized three linkers: 2-amino-1,1′-biphenyl-4,4′-dicarboxylic acid (H_2-NH_2-BPDC), 2-azido-1,1′-biphenyl-4,4′-dicarboxylic acid (H_2-N_3-BPDC), and 2-formyl-1,1′-biphenyl-4,4′-dicarboxylic acid (H_2-F-BPDC).[10,11] The formyl, azido, and amino groups were chosen because they are chemically orthogonal and can therefore be differentially addressed via postsynthetic modification reactions. We next examined whether bMOF-100 could withstand ligand-exchange reactions with the functionalized linkers. Crystalline samples of bMOF-100 were heated at 75 °C for 24 h in solutions of the individual linkers to prepare monofunctionalized materials. After reaction, the crystals are transparent (Figures S1−S3) and retain their crystallinity, as determined by powder X-ray diffraction (PXRD) (Figure S4). Thoroughly washed products were dissolved in deuterated acid and analyzed via proton nuclear magnetic resonance spectroscopy (^{1}H NMR) to determine the linker ratios and extent of exchange. 43.7%, 47.2%, and 50.3% of the BPDC linkers in bMOF-100 were replaced with NH_2-BPDC, N_3-BPDC, and F-BPDC, respectively (Figure S5). These results indicate that the linkers in bMOF-100 can be exchanged and that the crystal structure is compatible with the chosen functionalized linkers.

Having proven that bMOF-100 can be postsynthetically functionalized via ligand exchange, we next prepared its synthetically accessible analogue, N_3-bMOF-100, and performed ligand-exchange reactions to produce orthogonal binary functionalized MOFs. In trial ligand exchange reactions, we recognized that the N_3-BPDC linkers were much more labile than BPDC. We therefore determined that 35 °C was an optimal reaction temperature, permitting slower exchange and allowing for better control over the extent of ligand exchange. Using H_2-F-BPDC or H_2-NH_2-BPDC, the exchange percentage depends on the reaction time, as determined by ^{1}H NMR (Figures 2, S6, and S8). The MOF retains its crystallinity, as determined by PXRD (Figure 2B,E, S7, and S9). In both cases, the ratios of the two ligands (N_3-BPDC:F-BPDC or N_3-BPDC:NH_2-BPDC) can be varied within a broad range. Close analysis of the exchange percentages for the two ligands as a function of reaction time reveals different exchange behavior. In the case of F-BPDC exchange, there appears to be an upper limit of exchange (Figure 2C). Once the product crystal contains ~65% F-BPDC, no further exchange occurs. As the reaction time increases, the amount of crystals in the reaction visibly decreases. These observations suggest that if bMOF-100 contains too many F-BPDC ligands, it becomes thermodynamically unstable and eventually dissolves. A corollary to this observation is the F-

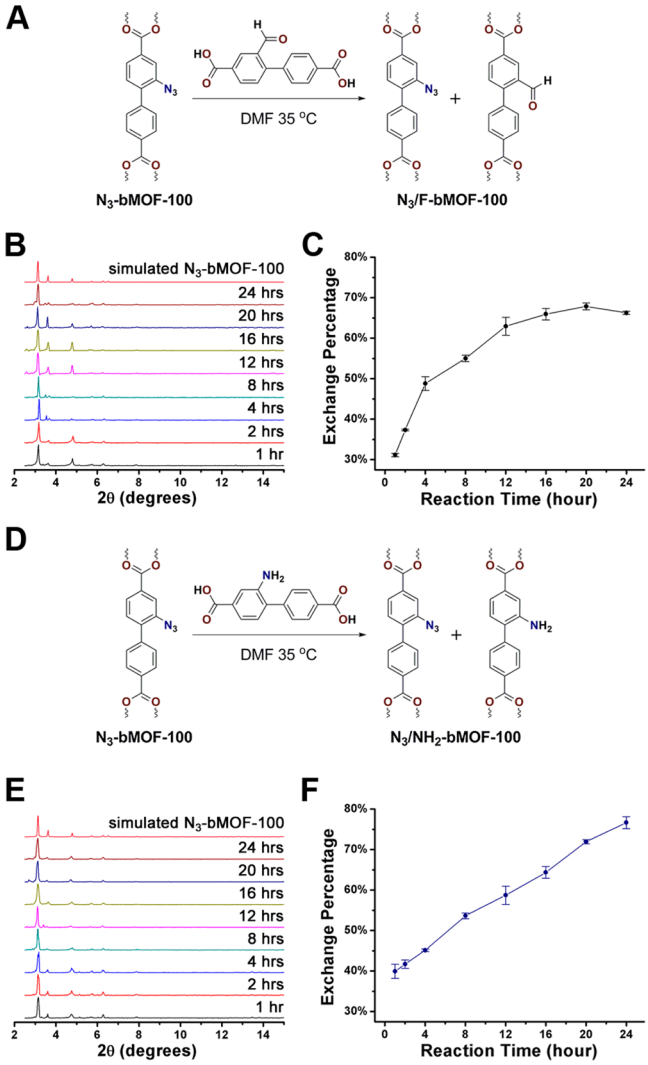

Figure 2. (A) Ligand-exchange reaction to produce N_3/F-bMOF-100. (B) PXRD comparing MOFs at different exchange time points with simulated pattern. (C) Percentage of F-BPDC in the product as determined by ^{1}H NMR. (D) Ligand-exchange reaction to produce N_3/NH_2-bMOF-100. (E) PXRD comparing MOFs at different exchange time points with simulated pattern. (F) Percentage of NH_2-BPDC in the product as determined by ^{1}H NMR.[12]

BPDC bMOF-100 analogue could not be prepared via direct synthesis. The NH_2-BPDC exchange reaction proceeds linearly with time (Figure 2F). No visible crystal dissolution was observed regardless of reaction time, suggesting that there is not an upper limit for NH_2-BPDC exchange.

As shown in Figure 2C, after 4 h of ligand exchange, the ratio of N_3-BPDC to F-BPDC in the product crystals is approximately 1:1. These crystals were reacted with H_2-NH_2-BPDC to create a ternary MOF with three orthogonal functional groups (Figure 3A). Similarly, 1:1 N_3-BPDC:NH_2-BPDC samples, which were synthesized according to Figure 2F, were reacted with H_2-F-BPDC (Figure 3D). By varying the reaction time, the final ligand composition is tunable, as determined by ^{1} H NMR (Figures 3C,F, S10, and S12), and the crystallinity is retained (Figure 3B,E, S11, and S13). N_3-BPDC is always present in the smallest amount, which suggests that it could be the most labile of the three linkers. The ligand present in the largest amount in the final product is always the third ligand that was introduced. Therefore,

DOI: 10.1021/jacs.5b06780
J. Am. Chem. Soc. 2015, 137, 10508−10511

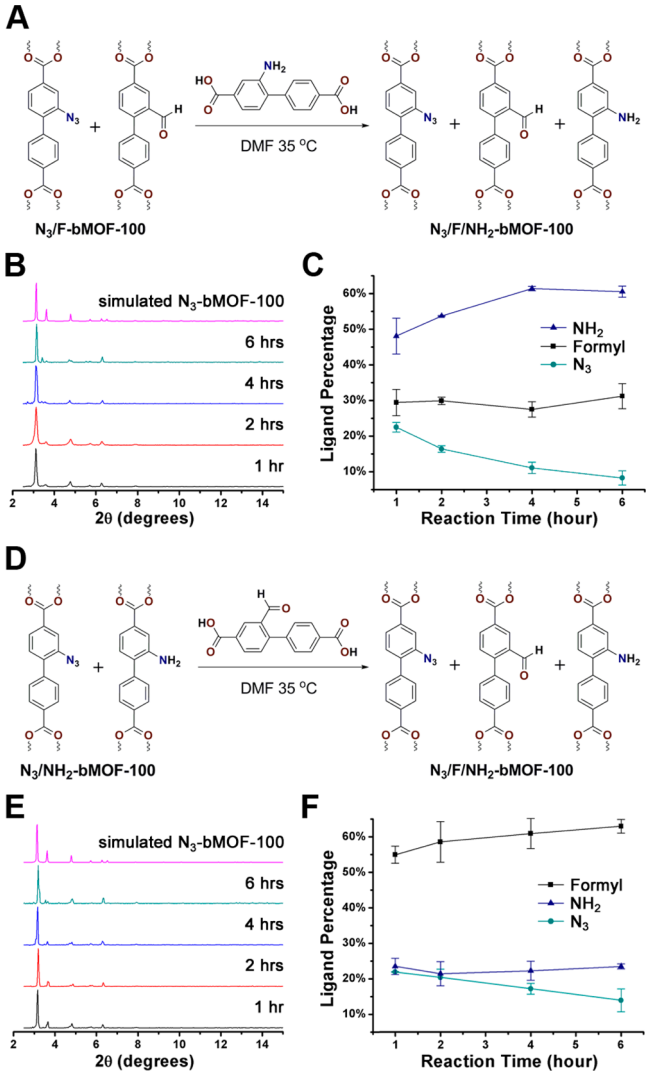

Figure 3. (A) Ligand -exchange reaction of N_3/F-bMOF-100 with H_2-NH_2-BPDC. (B) PXRD comparing MOFs at different exchange time points with simulated pattern. (C) Percentages of all three functionalized BPDC ligands in the product as determined by ^{1}H NMR. (D) Ligand-exchange reaction of N_3/NH_2-bMOF-100 with H_2-F-BPDC. (E) PXRD comparing MOFs at different exchange time points with simulated pattern. (F) Percentages of all three functionalized BPDC ligands in the product as determined by ^{1} H NMR. [14]

it can be concluded that the ligand composition is mainly kinetically controlled.

For a heterogeneous material with multiple functional groups, it is important to understand the spatial distribution of the different groups. Several methods have been established to study the linker distribution in MOFs, including microscopic attenuated total reflectance (ATR) infrared spectroscopy, photothermal induced resonance (PTIR), and solid-state NMR.[13] In the case of ligand exchange, knowing the spatial distribution of functional groups may allow one to retroactively understand aspects of the exchange process, such as whether particular ligands cluster together into domains or whether they are homogeneously distributed. Moreover, information about the ligand distribution will also be important for guiding the development of potential applications.

We used a dye-quencher approach to probe the distribution of two different functional groups. Using ~1:1 N_3-BPDC:F-BPDC difunctionalized bMOF-100 as a scaffold, we successively introduced a fluorescent group (carboxyrhodamine 110) via strain-promoted "click" chemistry[10,15] and then a fluorescence quencher (BHQ-1) via aldehyde-amine condensation[16] (Figure 4A). The cavities of bMOF-100 can accommodate these large

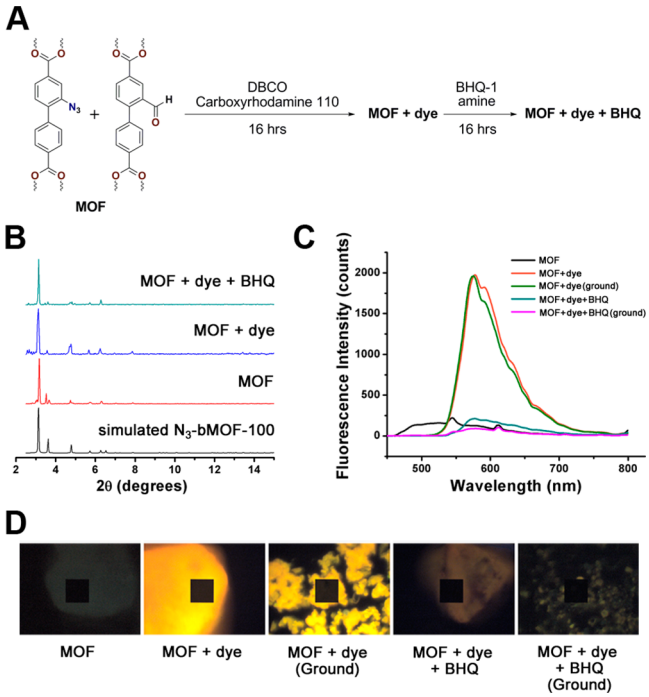

Figure 4. (A) Tandem postsynthetic modification reactions of ~1:1 N_3/F-bMOF-100 with dye and quencher molecules. (B) PXRD of modified MOFs compared to simulated pattern. (C) Fluorescence spectra (excited at 420 nm) of the MOF samples as determined by microspectrophotometry. (D) Images of MOF samples excited at 420 nm (black box: 31 × 31 μm sampling area for spectroscopy).

molecules (see Section 5.1 of Supporting Information, Figures S14−S15). After reaction with both dye and quencher, the MOF maintains its crystallinity (Figures 4B and S25). The crystals were copiously washed to remove unbound reactants, dissolved in dilute base, and then liquid chromatography-mass spectrometry (LC-MS) was used to analyze the contents of the dissolved MOF. This analysis revealed the presence of the BPDC linkers covalently modified with dye and quencher (see Section 5.2−5.6 of Supporting Information for complete details).

It is known that this dye-quencher pair needs to be ≤10 nm apart for FRET-based quenching.[17] Therefore, we reasoned that if the azido and formyl groups are organized apart from one another in discrete domains within the MOF, then most of the fluorophores would be sufficiently far from the quenchers and quenching would only occur at or near the interface between fluorophore and quencher domains. On the other hand, if the two groups were randomly distributed in the macroscopic crystal, nearly complete fluorescence quenching would be observed. In the case of ~1:1 binary functionalized bMOF-100, every zinc-adeninate cluster is connected by a three ligand bundle; therefore, there is a 75% chance that a dye and a quencher could be positioned in close proximity on two of these ligands. The modified MOF crystals were analyzed via microspectrophotometry (Figure 4C,D). In a typical experiment, MOF crystals were placed on a glass slide under the microspectrophotometer objective lens. The corresponding fluorescence spectra and

DOI: 10.1021/jacs.5b06780
J. Am. Chem. Soc. 2015, 137, 10508−10511

images were collected at the excitation wavelength of 420 nm. We observed almost complete fluorescence quenching in both intact crystals and ground samples (Figures 4, S26–S29). These results suggest that the dye and quencher, which mark the positions of the azido and formyl functional groups respectively, are not distributed in a core–shell fashion or clustered into relatively large discrete domains (≫10 nm), cases where effective quenching would be suppressed to some extent. Therefore, we conclude that the azido and formyl groups are likely randomly distributed in the crystal or clustered into small domains within 10 nm of each other.

We successfully realized mono-, di-, and trifunctionalization in a mesoporous MOF material, bMOF-100, via sequential postsynthetic ligand exchange reactions. The ratios of orthogonal functional groups are tunable with reaction time. We show that orthogonally functionalized crystals can be postsynthetically modified with large dye and quencher molecules to probe the distribution of functional moieties within the MOF. Spectrophotometric analysis of the dye-quencher MOFs suggests a random distribution of functional groups in binary functionalized bMOF-100. These results represent a significant step forward in the development of ordered hierarchically structured and functionalized 3D molecular materials.

■ ASSOCIATED CONTENT

Supporting Information

The Supporting Information is available free of charge on the ACS Publications website at DOI: 10.1021/jacs.5b06780.

Experimental details and additional data (PDF)

■ AUTHOR INFORMATION

Corresponding Author

*nrosi@pitt.edu

Notes

The authors declare no competing financial interest.

■ ACKNOWLEDGMENTS

Part of this work was performed under the RES contract DE-FE0004000 as part of the National Energy Technology Laboratory's Regional University Alliance (NETL-RUA), a collaborative initiative of the NETL. We thank the Petersen Nano Fabrication and Characterization Facility for access to PXRD and microspectrophotometry instrumentation and Ms. Disi Wang for help with figure preparation.

■ REFERENCES

(1) Zhou, H. C.; Long, J. R.; Yaghi, O. M. *Chem. Rev.* **2012**, *112*, 673.

(2) Furukawa, H.; Cordova, K. E.; O'Keeffe, M.; Yaghi, O. M. *Science* **2013**, *341*, 1230444.

(3) (a) Tanabe, K. K.; Cohen, S. M. *Chem. Soc. Rev.* **2011**, *40*, 498. (b) Cohen, S. M. *Chem. Rev.* **2012**, *112*, 970.

(4) (a) Burrows, A. D. *CrystEngComm* **2011**, *13*, 3623. (b) Kim, M.; Cahill, J. F.; Prather, K. A.; Cohen, S. M. *Chem. Commun.* **2011**, *47*, 7629. (c) Li, B.; Zhang, Y.; Ma, D.; Li, L.; Li, G.; Li, G.; Shi, Z.; Feng, S. *Chem. Commun.* **2012**, *48*, 6151. (d) Dau, P. V.; Cohen, S. M. *Inorg. Chem.* **2015**, *54*, 3134. (e) Li, B.; Chrzanowski, M.; Zhang, Y.; Ma, S. *Coord. Chem. Rev.* **2015**.

(5) (a) Karagiaridi, O.; Bury, W.; Mondloch, J. E.; Hupp, J. T.; Farha, O. K. *Angew. Chem., Int. Ed.* **2014**, *53*, 4530. (b) Han, Y.; Li, J. R.; Xie, Y.; Guo, G. *Chem. Soc. Rev.* **2014**, *43*, 5952. (c) Deria, P.; Mondloch, J. E.; Karagiaridi, O.; Bury, W.; Hupp, J. T.; Farha, O. K. *Chem. Soc. Rev.* **2014**, *43*, 5896. (d) Burnett, B. J.; Barron, P. M.; Hu, C.; Choe, W. *J. Am. Chem. Soc.* **2011**, *133*, 9984. (e) Karagiaridi, O.; Bury, W.; Sarjeant, A. A.; Stern, C. L.; Farha, O. K.; Hupp, J. T. *Chem. Sci.* **2012**, *3*, 3256. (f) Kim, M.; Cahill, J. F.; Su, Y.; Prather, K. A.; Cohen, S. M. *Chem. Sci.* **2012**, *3*, 126. (g) Kim, M.; Cahill, J. F.; Fei, H.; Prather, K. A.; Cohen, S. M. *J. Am. Chem. Soc.* **2012**, *134*, 18082. (h) Karagiaridi, O.; Lalonde, M. B.; Bury, W.; Sarjeant, A. A.; Farha, O. K.; Hupp, J. T. *J. Am. Chem. Soc.* **2012**, *134*, 18790. (i) Takaishi, S.; DeMarco, E. J.; Pellin, M. J.; Farha, O. K.; Hupp, J. T. *Chem. Sci.* **2013**, *4*, 1509. (j) Kim, S.; Dawson, K. W.; Gelfand, B. S.; Taylor, J. M.; Shimizu, G. K. *J. Am. Chem. Soc.* **2013**, *135*, 963. (k) Jeong, S.; Kim, D.; Song, X.; Choi, M.; Park, N.; Lah, M. S. *Chem. Mater.* **2013**, *25*, 1047. (l) Bury, W.; Fairen-Jimenez, D.; Lalonde, M. B.; Snurr, R. Q.; Farha, O. K.; Hupp, J. T. *Chem. Mater.* **2013**, *25*, 739. (m) Fei, H.; Cahill, J. F.; Prather, K. A.; Cohen, S. M. *Inorg. Chem.* **2013**, *52*, 4011. (n) Gross, A. F.; Sherman, E.; Mahoney, S. L.; Vajo, J. J. *J. Phys. Chem. A* **2013**, *117*, 3771. (o) Hirai, K.; Chen, K.; Fukushima, T.; Horike, S.; Kondo, M.; Louvain, N.; Kim, C.; Sakata, Y.; Meilikhov, M.; Sakata, O.; Kitagawa, S.; Furukawa, S. *Dalton Trans.* **2013**, *42*, 15868. (p) Li, T.; Kozlowski, M. T.; Doud, E. A.; Blakely, M. N.; Rosi, N. L. *J. Am. Chem. Soc.* **2013**, *135*, 11688. (q) Karagiaridi, O.; Bury, W.; Tylianakis, E.; Sarjeant, A. A.; Hupp, J. T.; Farha, O. K. *Chem. Mater.* **2013**, *25*, 3499. (r) Hong, D. H.; Suh, M. P. *Chem. - Eur. J.* **2014**, *20*, 426. (s) Fei, H.; Shin, J.; Meng, Y. S.; Adelhardt, M.; Sutter, J.; Meyer, K.; Cohen, S. M. *J. Am. Chem. Soc.* **2014**, *136*, 4965. (t) Jeong, S.; Kim, D.; Shin, S.; Moon, D.; Cho, S. J.; Lah, M. S. *Chem. Mater.* **2014**, *26*, 1711. (u) Szilágyi, P. Á.; Weinrauch, I.; Oh, H.; Hirscher, M.; Juan-Alcañiz, J.; Serra-Crespo, P.; de Respinis, M.; Trześniewski, B. J.; Kapteijn, F.; Geerlings, H.; Gascon, J.; Dam, B.; Grzech, A.; van de Krol, R.; Geerlings, H. *J. Phys. Chem. C* **2014**, *118*, 19572. (v) Morabito, J. V.; Chou, L. Y.; Li, Z.; Manna, C. M.; Petroff, C. A.; Kyada, R. J.; Palomba, J. M.; Byers, J. A.; Tsung, C. K. *J. Am. Chem. Soc.* **2014**, *136*, 12540. (w) Fei, H.; Pullen, S.; Wagner, A.; Ott, S.; Cohen, S. M. *Chem. Commun.* **2015**, *51*, 66. (x) Yuan, S.; Lu, W.; Chen, Y. P.; Zhang, Q.; Liu, T. F.; Feng, D.; Wang, X.; Qin, J.; Zhou, H. C. *J. Am. Chem. Soc.* **2015**, *137*, 3177. (y) Fei, H.; Cohen, S. M. *J. Am. Chem. Soc.* **2015**, *137*, 2191. (z) Zhao, J.; Li, H.; Han, Y.; Li, R.; Ding, X.; Feng, X.; Wang, B. *J. Mater. Chem. A* **2015**, *3*, 12145.

(6) (a) Furukawa, H.; Muller, U.; Yaghi, O. M. *Angew. Chem., Int. Ed.* **2015**, *54*, 3417. (b) Guillerm, V.; Kim, D.; Eubank, J. F.; Luebke, R.; Liu, X.; Adil, K.; Lah, M. S.; Eddaoudi, M. *Chem. Soc. Rev.* **2014**, *43*, 6141.

(7) Valtchev, V.; Majano, G.; Mintova, S.; Perez-Ramirez, J. *Chem. Soc. Rev.* **2013**, *42*, 263.

(8) (a) Xuan, W.; Zhu, C.; Liu, Y.; Cui, Y. *Chem. Soc. Rev.* **2012**, *41*, 1677. (b) Song, L.; Zhang, J.; Sun, L.; Xu, F.; Li, F.; Zhang, H.; Si, X.; Jiao, C.; Li, Z.; Liu, S.; Liu, Y.; Zhou, H.; Sun, D.; Du, Y.; Cao, Z.; Gabelica, Z. *Energy Environ. Sci.* **2012**, *5*, 7508.

(9) An, J.; Farha, O. K.; Hupp, J. T.; Pohl, E.; Yeh, J. I.; Rosi, N. L. *Nat. Commun.* **2012**, *3*, 604.

(10) Liu, C.; Li, T.; Rosi, N. L. *J. Am. Chem. Soc.* **2012**, *134*, 18886.

(11) Burrows, A. D.; Frost, C. G.; Mahon, M. F.; Richardson, C. *Angew. Chem., Int. Ed.* **2008**, *47*, 8482.

(12) Error bars in Figure 2C,F are standard deviations of two parallel sets of experiments.

(13) (a) Furukawa, S.; Hirai, K.; Takashima, Y.; Nakagawa, K.; Kondo, M.; Tsuruoka, T.; Sakata, O.; Kitagawa, S. *Chem. Commun.* **2009**, 5097. (b) Kong, X.; Deng, H.; Yan, F.; Kim, J.; Swisher, J. A.; Smit, B.; Yaghi, O. M.; Reimer, J. A. *Science* **2013**, *341*, 882. (c) Katzenmeyer, A. M.; Canivet, J.; Holland, G.; Farrusseng, D.; Centrone, A. *Angew. Chem., Int. Ed.* **2014**, *53*, 2852. (d) Krajnc, A.; Kos, T.; Zabukovec Logar, N.; Mali, G. *Angew. Chem., Int. Ed.* **2015**.

(14) Error bars in Figure 3C,F are standard deviations of two parallel sets of experiments.

(15) (a) Jewett, J. C.; Bertozzi, C. R. *Chem. Soc. Rev.* **2010**, *39*, 1272. (b) Wang, Z.; Liu, J.; Arslan, H. K.; Grosjean, S.; Hagendorn, T.; Gliemann, H.; Brase, S.; Woll, C. *Langmuir* **2013**, *29*, 15958. (c) Morris, W.; Briley, W. E.; Auyeung, E.; Cabezas, M. D.; Mirkin, C. A. *J. Am. Chem. Soc.* **2014**, *136*, 7261.

(16) Morris, W.; Doonan, C. J.; Furukawa, H.; Banerjee, R.; Yaghi, O. M. *J. Am. Chem. Soc.* **2008**, *130*, 12626.

(17) (a) Förster, T. *Ann. Phys. (Berlin, Ger.)* **1948**, *437*, 55. (b) Lee, C. Y.; Farha, O. K.; Hong, B. J.; Sarjeant, A. A.; Nguyen, S. T.; Hupp, J. T. *J. Am. Chem. Soc.* **2011**, *133*, 15858.

DOI: 10.1021/jacs.5b06780
J. Am. Chem. Soc. 2015, 137, 10508–10511